

Nonlinear Feedback Control of Axisymmetric Aerial Vehicles

Daniele Pucci¹, Tarek Hamel², Pascal Morin^{3*}, Claude Samson⁴

¹ Italian Institute of Technology, Genova, Italy, daniele.pucci@iit.it

² I3S/UNSA, Sophia-Antipolis, France, thamel@i3s.unice.fr

³ ISIR-UPMC, Paris, France, morin@isir.upmc.fr

⁴ INRIA, I3S/UNSA, Sophia Antipolis, France, claude.samson@inria.fr, csamson@i3s.unice.fr

March 24, 2014

Abstract

We investigate the use of simple aerodynamic models for the feedback control of aerial vehicles with large flight envelopes. Thrust-propelled vehicles with a body shape symmetric with respect to the thrust axis are considered. Upon a condition on the aerodynamic characteristics of the vehicle, we show that the equilibrium orientation can be explicitly determined as a function of the desired flight velocity. This allows for the adaptation of previously proposed control design approaches based on the thrust direction control paradigm. Simulation results conducted by using measured aerodynamic characteristics of quasi-axisymmetric bodies illustrate the soundness of the proposed approach.

1 Introduction

Alike other engineering fields, flight control makes extensive use of linear control techniques [41]. One reason is the existence of numerous tools to assess the robustness properties of a linear feedback controller [36] (gain margin, phase margin, H_2 , H_∞ , or LMI techniques, etc.). Another reason is that flight control techniques have been developed primarily for full-size commercial airplanes that are designed and optimized to fly along very specific trajectories (trim trajectories with a very narrow range of angles of attack). Control design is then typically achieved from the linearized equations of motion along desired trajectories. However, some aerial vehicles are required to fly in very diverse conditions that involve large and rapid variations of the angle of attack. Examples are given by fighter aircraft, convertible aircraft, or small Unmanned Aerial vehicles (UAVs) operating in windy environments. As a matter of fact, some Vertical Take-Off and Landing (VTOL) vehicles, like e.g. ducted fans, are often subjected to large variations of the angle of attack when transitioning from hover to horizontal cruising flight. It then matters to ensure large stability domains that are achievable via the use of nonlinear feedback designs.

Nonlinear feedback control of aircraft can be traced back to the early eighties. Following [39], control laws based on the dynamic inversion technique have been proposed to extend the flight envelope of military aircraft (see, e.g., [43] and the references therein). The control design strongly relies on tabulated models of aerodynamic forces and moments, like the High-Incidence Research Model (HIRM) of the Group for Aeronautical Research and Technology in Europe (GARTEUR) [25]. Compared to linear techniques, this type of approach allows one to extend the flight domain without involving gain scheduling strategies. The angle of attack is assumed to remain away from the stall zone. However, should this assumption be violated the system's behavior is unpredictable. Comparatively, nonlinear feedback control of VTOL vehicles is more recent, but it has been addressed with a larger variety of techniques. Besides dynamic inversion [10], other techniques include Lyapunov-based design [24, 15], Backstepping [3], Sliding modes [3, 45], and Predictive control [19, 2]. A more complete bibliography on this topic can be found in [13]. Since most of these studies address the stabilization of hover flight or low-velocity trajectories, little attention has been paid to aerodynamic effects. These are typically either ignored or modeled as a simple additive perturbation, the effect of which has to be compensated for by the feedback action. In highly dynamic flight or harsh wind conditions, however, aerodynamic effects become important. This raises several questions, seldom addressed so far

*Corresponding author

by the control and robotics communities, such as, e.g., *which models of aerodynamic effects should be considered for the control design?* or *which feedback control solutions can be inferred from these models so as to ensure large stability domains and robustness?*

Classical methods used in aerodynamic modelling to precisely describe aerodynamic forces, e.g. computational fluid dynamics (CFD) or wind tunnel measurements, do not provide analytical expressions of aerodynamic characteristics. From a control design perspective they are useful to finely tune a controller around a given flight velocity, but exploiting them in the case of large flight envelopes (i.e., that involve strong variations of either the flight velocity or the angle of attack) is difficult. In this paper we advocate the use of simple analytical models of aerodynamic characteristics. Although relatively imprecise, these models may account for important structural properties of the system in a large flight envelope. The main idea is to exploit these properties at the control design level and rely on the robustness of feedback controllers to cope with discrepancies between the model and the true aerodynamic characteristics. More precisely, for the class of vehicles with a body-shape symmetric w.r.t. the thrust axis, we provide conditions on the aerodynamic coefficients under which the vehicle's equilibrium orientation associated with a desired flight velocity is explicitly (and uniquely) defined. We also show that such conditions are satisfied by simple models that approximate at the first order aerodynamic characteristics of real systems reported in the literature. The control design then essentially consists in aligning the thrust direction with the desired equilibrium orientation and monitoring the thrust intensity to compensate for the intensity of external forces. This corresponds to the thrust direction control paradigm, which has been exploited for VTOL vehicles either by neglecting aerodynamic effects [8], or by considering systems submitted to drag forces only [12]. Although the determination of the vehicle's equilibrium orientation is straightforward in these cases, this is a major issue for more general vehicles (see [34] for more details). By showing that the thrust direction control paradigm can be extended to aerial vehicles submitted to significant lift forces, this paper makes a step towards a unified control approach for both VTOL vehicles and airplanes.

The paper is organized as follows. Section 2 provides the notation and background. In Section 3, we show that for a class of symmetric bodies the dynamical equations of motion can be transformed into a simpler form that allows one to explicitly determine the equilibrium orientation associated with a desired flight velocity. This transformation is then used in Section 4 to propose a feedback control design method applicable to several vehicles of interest.

2 Notation and background

Throughout the paper, \mathbf{E}^3 denotes the 3D Euclidean vector space and vectors in \mathbf{E}^3 are denoted with bold letters. Inner and cross products in \mathbf{E}^3 are denoted by the symbols \cdot and \times respectively.

Let $\mathcal{I} = \{O; \mathbf{i}_0, \mathbf{j}_0, \mathbf{k}_0\}$ denote a fixed inertial frame with respect to (w.r.t.) which the vehicle's absolute pose is measured (see Figure 1). This frame is chosen as the NED frame (North-East-Down) with \mathbf{i}_0 pointing to the North, \mathbf{j}_0 pointing to the East, and \mathbf{k}_0 pointing to the center of the Earth. Let $\mathcal{B} = \{G; \mathbf{i}, \mathbf{j}, \mathbf{k}\}$ denote a frame attached to the body, with G the body's center of mass. The linear and angular velocities \mathbf{v} and $\boldsymbol{\omega}$ of the body frame \mathcal{B} are then defined by

$$\mathbf{v} := \frac{d}{dt} \mathbf{OG} , \quad \frac{d}{dt} (\mathbf{i}, \mathbf{j}, \mathbf{k}) := \boldsymbol{\omega} \times (\mathbf{i}, \mathbf{j}, \mathbf{k}) , \quad (1)$$

where, here and throughout the paper, the time-derivative is taken w.r.t. the inertial frame \mathcal{I} .

2.1 Equations of motion

Let \mathbf{F} and \mathbf{M} denote respectively the resultant of control and external forces acting on a rigid body of mass m and the moment of these forces about the body's center of mass G . Newton's and Euler's theorems of Mechanics state that

$$\dot{\mathbf{q}} = \mathbf{F} , \quad \dot{\mathbf{h}} = \mathbf{M} , \quad (2)$$

with

$$\mathbf{q} := m\mathbf{v} , \quad \mathbf{h} := - \int_{P' \in \text{body}} \mathbf{GP}' \times (\mathbf{GP}' \times \boldsymbol{\omega}) \, dm = \mathbf{J}\boldsymbol{\omega} , \quad (3)$$

where \mathbf{J} denotes the inertia operator at G . Throughout this paper aircraft are modeled as rigid bodies of constant mass and we focus on the class of vehicles controlled via four control inputs, namely the thrust intensity $T \in \mathbb{R}$ of a body-fixed thrust force $\mathbf{T} = -T\mathbf{k}$ and the three components (in body-frame) of a control torque vector $\boldsymbol{\Gamma}_G$. This

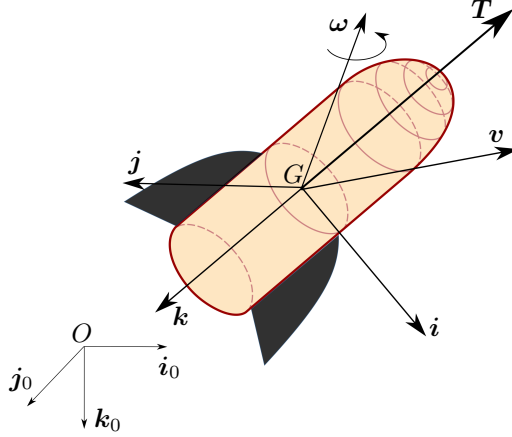


Figure 1: Notation.

class of systems covers (modulo an adequate choice of control inputs) a large variety of aerial vehicles of interest, like multi-copters, helicopters, convertibles UAVs, or even conventional airplanes. The torque actuation can be obtained in various ways by using, e.g., control surfaces (fixed-wing aircraft), propellers (multi-copters), swash-plate mechanisms and tail-rotors (helicopters). By neglecting round-earth effects and buoyancy forces¹, control and external forces and moments acting on the aircraft are commonly modeled as follows [7, Ch. 2], [12], [40], [41]:

$$\begin{aligned} \mathbf{F} &= m\mathbf{g} + \mathbf{F}_a - T\mathbf{k} + \mathbf{F}_b, \\ \mathbf{M} &= \mathbf{G}\mathbf{P} \times \mathbf{F}_a + T\mathbf{k} \times \mathbf{G}\Theta + \mathbf{\Gamma}_G, \end{aligned} \quad (4)$$

where $\mathbf{g} = g\mathbf{k}_0$ is the gravitational acceleration vector, (\mathbf{F}_a, P) is the resultant of the aerodynamic forces and its point of application², and Θ is the point of application of the thrust force. In Eq. (4) we assume that the gyroscopic torque (usually associated with rotary-wing aircraft) is negligible or that it has already been compensated for via a preliminary torque control action. The force \mathbf{F}_b is referred to as a *body force*. It is induced by the control torque vector $\mathbf{\Gamma}_G$ and thus represents the effect of the control torque actuation on the position dynamics. The term $T\mathbf{k} \times \mathbf{G}\Theta$ in (4) represents the effect of the control force actuation on the orientation dynamics.

Beside the gravitational force, Eq. (4) allows one to identify three types of forces (and torques): *i) control forces*, *ii) body forces*, which cover coupling effects between thrust and torque actuations, and *iii) aerodynamic forces*. This decomposition is based on a separation principle that is only valid in the first approximation. Nevertheless, identifying the dominant terms is useful from a control point of view to work out generic control strategies that can be refined on a case by case basis for specific classes of vehicles. A more detailed discussion of the modelling of body and aerodynamic forces follows.

2.2 Body forces

The influence of the torque control inputs on the translational dynamics via the body force \mathbf{F}_b depends on the torque generation mechanism. More specifically, this coupling term is negligible for quadrotors [9], [31], [4], but it can be significant for helicopters due to the swashplate mechanism [11, Ch.1], [6], [21], [23], [27, Ch. 5], and for ducted-fan tail-sitters due to the rudder system [28, Ch. 3], [30]. Thus, the relevance of this body force must be discussed in relation to the specific application [30] [28, Ch. 3] [13]. Note, however, that the body force \mathbf{F}_b is typically small compared to either the gravitational force, the aerodynamic force, or the thrust force. Similarly, the term $T\mathbf{k} \times \mathbf{G}\Theta$ in (4), which reflects the influence of the thrust control input on the rotational dynamics, is usually small because Θ is close to the axis (G, \mathbf{k}) . Assuming that body forces and corresponding torques can be either neglected or compensated for by control actions, we focus hereafter on the modelling of aerodynamic forces acting on the vehicle's main body.

¹The aircraft is assumed to be much heavier than air.

²The point P is the so called *body's center of pressure*.

2.3 Aerodynamic forces

The modelling of aerodynamic forces and torques \mathbf{F}_a and $\mathbf{M}_a := \mathbf{GP} \times \mathbf{F}_a$ acting on the vehicle is of particular importance. Results on this topic can be found in [1] [40, Ch. 2] [41, Ch. 2] for fixed-wing aircraft, in [14] [4] for quadrotors, in [16] [20] [26] [28, Ch. 3] [29] for ducted-fan tail-sitters, and in [32], [42] for helicopters. The notation for aerodynamic forces used throughout this paper is presented next.

Denote by \mathbf{v}_a the *air velocity*, which is defined as the difference between \mathbf{v} and wind's velocity \mathbf{v}_w , i.e. $\mathbf{v}_a = \mathbf{v} - \mathbf{v}_w$. The *lift force* \mathbf{F}_L is the aerodynamic force component perpendicular to the air velocity, and the *drag force* \mathbf{F}_D is the aerodynamic force component along the air velocity's direction. Now, consider a (any) pair of angles (α, β) characterizing the orientation of \mathbf{v}_a with respect to the body frame (e.g. Figure 3). Combining the *Buckingham π -theorem* [1, p. 34] with the knowledge that the intensity of the *steady* aerodynamic force varies approximately like the square of the air speed $|\mathbf{v}_a|$ yields the existence of two dimensionless functions $C_L(\cdot)$ and $C_D(\cdot)$ depending on the *Reynolds number* R_e , the *Mach number* M , and (α, β) , and such that

$$\begin{aligned} \mathbf{F}_a &= \mathbf{F}_L + \mathbf{F}_D, \\ \mathbf{F}_L &= k_a |\mathbf{v}_a| C_L(R_e, M, \alpha, \beta) \mathbf{r}(\alpha, \beta, |\mathbf{v}_a|) \times \mathbf{v}_a, \\ \mathbf{F}_D &= -k_a |\mathbf{v}_a| C_D(R_e, M, \alpha, \beta) \mathbf{v}_a, \\ \mathbf{r} \cdot \mathbf{v}_a &= 0, \quad |\mathbf{r}| = 1, \\ k_a &:= \rho \Sigma / 2, \end{aligned} \tag{5}$$

with ρ the *free stream* air density, Σ an area germane to the given body shape, $\mathbf{r}(\cdot)$ a unit vector-valued function, $C_D (\in \mathbb{R}^+)$ and $C_L (\in \mathbb{R})$ the *aerodynamic characteristics* of the body, i.e. the so-called *drag coefficient* and *lift coefficient*, respectively. In view of the above representation of the aerodynamic force – first introduced in [35] – the lift direction is independent from the aerodynamic coefficients, which in turn characterize the aerodynamic force intensity since $|\mathbf{F}_a| = k_a |\mathbf{v}_a|^2 \sqrt{C_L^2 + C_D^2}$. The lift direction is fully characterized by the unitary vector $\mathbf{r}(\cdot)$, which only depends on (α, β) and on the air velocity magnitude $|\mathbf{v}_a|$. We will see further on that axisymmetry of the vehicle's body yields a specific expression of the vector $\mathbf{r}(\cdot)$. By considering the model (5), we implicitly neglect the effects of the vehicle's *rotational and unsteady motions* on its surrounding airflow (see [40, p. 199] for more details).

2.4 Control model

With the assumptions and simplifications discussed above, the control model reduces to

$$m\dot{\mathbf{v}} = m\mathbf{g} + \mathbf{F}_a - T\mathbf{k}, \tag{6a}$$

$$\frac{d}{dt}(\mathbf{i}, \mathbf{j}, \mathbf{k}) = \boldsymbol{\omega} \times (\mathbf{i}, \mathbf{j}, \mathbf{k}), \tag{6b}$$

$$\frac{d}{dt}(\mathbf{J}\boldsymbol{\omega}) = \mathbf{GP} \times \mathbf{F}_a + \boldsymbol{\Gamma}_G. \tag{7}$$

To develop general control principles that apply to a large number of aerial vehicles, one must get free of actuation specificities and concentrate on the vehicle's governing dynamics. In agreement with a large number of works on VTOL control (see [13] for a survey) and in view of Eq. (7), which points out how $\boldsymbol{\omega}$ can be modified via the choice of the control torque $\boldsymbol{\Gamma}_G$, a complementary assumption consists in considering the angular velocity $\boldsymbol{\omega}$ as an intermediate control input. This implicitly means that the control torque calculation and production can be done independently of high-level control objectives, at least in the first design stage. The corresponding physical assumption is that “almost” any desired angular velocity can be obtained after a short transient time. In the language of Automatic Control, this is a typical “backstepping” assumption. Once it is made, the vehicle's actuation consists in four input variables, namely, the thrust intensity and the three components of $\boldsymbol{\omega}$. The control model then reduces to Eqs. (6), with T and $\boldsymbol{\omega}$ as control inputs.

3 Symmetric bodies and spherical equivalence

Eq. (6) shows how the gravitational force $m\mathbf{g}$ and the aerodynamic force \mathbf{F}_a take part in the body's linear acceleration vector. It also shows that, for the body to move with a constant velocity, the controlled thrust vector $T\mathbf{k}$ must be equal to the resultant external force

$$\mathbf{F}_{ext} := m\mathbf{g} + \mathbf{F}_a.$$

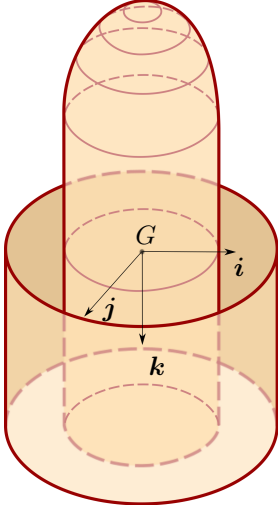


Figure 2: Symmetric and bisymmetric shapes

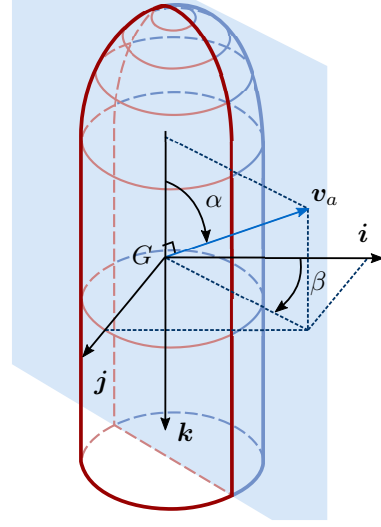


Figure 3: The (α, β) angles.

When \mathbf{F}_a does not depend on the vehicle's orientation, as in the case of *spherical bodies* (see [11] for details), the resultant external force \mathbf{F}_{ext} does not depend on this orientation either. The thrust direction at the equilibrium is then unique and it is explicitly given by the direction of \mathbf{F}_{ext} . The control strategy then basically consists in aligning the thrust direction \mathbf{k} with the direction of \mathbf{F}_{ext} (using $\boldsymbol{\omega}$ as control input) and in opposing the thrust magnitude to the intensity of \mathbf{F}_{ext} (using the thrust T as control input). This is the basic principle of the thrust direction control paradigm [8, 12]. For most vehicles encountered in practice, however, aerodynamic forces depend on the vehicle's orientation, and thus on the direction of \mathbf{k} . In particular, the equilibrium relation $T\mathbf{k} = \mathbf{F}_{ext}$ then becomes an implicit equation with both sides of this equality depending on \mathbf{k} . In this case, existence, uniqueness, and explicit determination of the equilibrium thrust direction(s) become fundamental questions for the control design [34]. In this section, we provide answers to these questions for a class of axisymmetric vehicles, in the continuity of [34], [35], where axisymmetry is shown to infer geometrical aerodynamic properties that simplify the associated control problem. More precisely, let us consider vehicles whose external surface \mathcal{S} is characterized by the existence of an orthonormal body frame $\mathcal{B}_c = \{G_c; \mathbf{i}, \mathbf{j}, \mathbf{k}\}$ that satisfies either one of the following assumptions:

Assumption 1 (Symmetry) Any point $P \in \mathcal{S}$ transformed by the rotation of an angle θ about the axis $G_c\mathbf{k}$, i.e. by the operator defined by $g_\theta(\cdot) = \text{rot}_{G_c\mathbf{k}}(\theta)(\cdot)$, also belongs to \mathcal{S} , i.e. $g_\theta(P) \in \mathcal{S}$.

Assumption 2 (Bisymmetry) Any point $P \in \mathcal{S}$ transformed by the composition of two rotations of angles θ and π about the axes $G_c\mathbf{k}$ and $G_c\mathbf{j}$, i.e. by the operator defined by $g_\theta(\cdot) = (\text{rot}_{G_c\mathbf{k}}(\theta) \circ \text{rot}_{G_c\mathbf{j}}(\pi))(\cdot)$, also belongs to \mathcal{S} , i.e. $g_\theta(P) \in \mathcal{S}$.

The operator $\text{rot}_{O\mathbf{v}}(\psi)(P)$ stands for the rotation about the axis $O\mathbf{v}$ by the angle ψ of the point P . Examples of “symmetric” and “bisymmetric” shapes satisfying these assumptions are represented in Figure 2 (with $G = G_c$). Note that various human-made aerial devices (rockets, missiles, airplanes with annular wings, etc.) satisfy the symmetry property of Assumption 1 in the first approximation, and that the present study is thus of direct relevance for the modelling and control of these devices. For symmetric shapes, i.e. such that Assumption 1 holds true, one can define $\alpha \in [0, \pi]$ as the *angle of attack*³ between $-\mathbf{k}$ and \mathbf{v}_a , and $\beta \in (-\pi, \pi]$ as the angle between the unit frame vector \mathbf{i} and the projection of \mathbf{v}_a on the plane $\{G_c; \mathbf{i}, \mathbf{j}\}$ (see Figure 3). Observe that this assumption also implies that:

P1 : the aerodynamic force \mathbf{F}_a does not change when the body rotates about its axis of symmetry $G_c\mathbf{k}$;

P2 : $\mathbf{F}_a \in \text{span}\{\mathbf{k}, \mathbf{v}_a\}$.

Property P1 in turn implies that the aerodynamic characteristics do not depend on β , whereas Property P2 implies that

³The angle of attack α so defined does not coincide with that used for airplanes equipped with planar wings, which break the body's rotational symmetry about $G_c\mathbf{k}$ [40, p. 53].

- i) the unit vector \mathbf{r} in (5) is orthogonal to \mathbf{k} and independent of the angle of attack α ;
- ii) the lift coefficient is equal to zero when $\alpha = \{0, \pi\}$.

Subsequently, the expressions (5) of the lift and drag forces specialize to

$$\begin{aligned}\mathbf{F}_L &= k_a |\mathbf{v}_a| C_L(R_e, M, \alpha) \mathbf{r}(\beta) \times \mathbf{v}_a, \\ \mathbf{F}_D &= -k_a |\mathbf{v}_a| C_D(R_e, M, \alpha) \mathbf{v}_a, \\ \mathbf{r}(\beta) &= -\sin(\beta) \mathbf{i} + \cos(\beta) \mathbf{j}.\end{aligned}\tag{8}$$

Under the stronger Assumption 2, i.e. when the body's shape is also π -symmetric w.r.t. the $G_c \mathbf{j}$ axis, the aerodynamic characteristics C_L and C_D must be π -periodic w.r.t. α . The aforementioned choice of (α, β) implies that

$$\alpha = \cos^{-1} \left(-\frac{v_{a3}}{|\mathbf{v}_a|} \right), \quad \beta = \text{atan2}(v_{a2}, v_{a1}),\tag{9}$$

and

$$\begin{aligned}v_{a1} &= |\mathbf{v}_a| \sin(\alpha) \cos(\beta), \\ v_{a2} &= |\mathbf{v}_a| \sin(\alpha) \sin(\beta), \\ v_{a3} &= -|\mathbf{v}_a| \cos(\alpha).\end{aligned}\tag{10}$$

with v_{a_i} ($i = 1, 2, 3$) denoting the coordinates of \mathbf{v}_a in the body-fixed frame basis. From the definitions of α and $\mathbf{r}(\beta)$, one then verifies that

$$\mathbf{r}(\beta) \times \mathbf{v}_a = -\cot(\alpha) \mathbf{v}_a - \frac{|\mathbf{v}_a|}{\sin(\alpha)} \mathbf{k},$$

so that $\mathbf{F}_a = \mathbf{F}_L + \mathbf{F}_D$ becomes

$$\mathbf{F}_a = -k_a |\mathbf{v}_a| \left[\left(C_D(\cdot) + C_L(\cdot) \cot(\alpha) \right) \mathbf{v}_a + \frac{C_L(\cdot)}{\sin(\alpha)} |\mathbf{v}_a| \mathbf{k} \right].\tag{11}$$

For constant Reynolds and Mach numbers the aerodynamic coefficients depend only on α and one readily deduces the following result from (11).

Proposition 1 ([35], [34]) *Consider an axisymmetric thrust-propelled vehicle subjected to aerodynamic forces given by (8). Assume that the aerodynamic coefficients satisfy the following relation*

$$C_D(\alpha) + C_L(\alpha) \cot(\alpha) = C_{D_0},\tag{12}$$

with C_{D_0} denoting a constant number. Then, Eq. (6) can also be written as

$$m\dot{\mathbf{v}} = m\mathbf{g} + \mathbf{F}_p - T_p \mathbf{k},\tag{13}$$

with

$$T_p = T + k_a |\mathbf{v}_a|^2 \frac{C_L(\alpha)}{\sin(\alpha)},\tag{14a}$$

$$\mathbf{F}_p(\mathbf{v}_a) = -k_a C_{D_0} |\mathbf{v}_a| \mathbf{v}_a.\tag{14b}$$

This proposition points out the possibility of seeing an axisymmetric body subjected to both drag and lift forces as a sphere subjected to the orientation independent drag force \mathbf{F}_p and powered by the thrust force $\mathbf{T}_p = -T_p \mathbf{k}$.

It follows from (13) that given a desired reference velocity \mathbf{v}_r , there exists a unique (up to sign) equilibrium thrust direction \mathbf{k}_{ref} as long as $|m\mathbf{g} + \mathbf{F}_p - m\dot{\mathbf{v}}_r| \neq 0$ along this reference velocity. In particular, this direction is explicitly defined by

$$\mathbf{k}_{ref} = \frac{m\mathbf{g} + \mathbf{F}_p(\mathbf{v}_{r,a}) - m\dot{\mathbf{v}}_r}{|m\mathbf{g} + \mathbf{F}_p(\mathbf{v}_{r,a}) - m\dot{\mathbf{v}}_r|}$$

where $\mathbf{v}_{r,a} = \mathbf{v}_r - \mathbf{v}_w$. The main condition for this result to hold is that the relation (12) must be satisfied. Obviously, this condition is compatible with an infinite number of functions C_D and C_L . Let us point out a particular set of simple functions that also satisfy the π -periodicity property w.r.t. the angle of attack α associated with *bisymmetric* bodies.

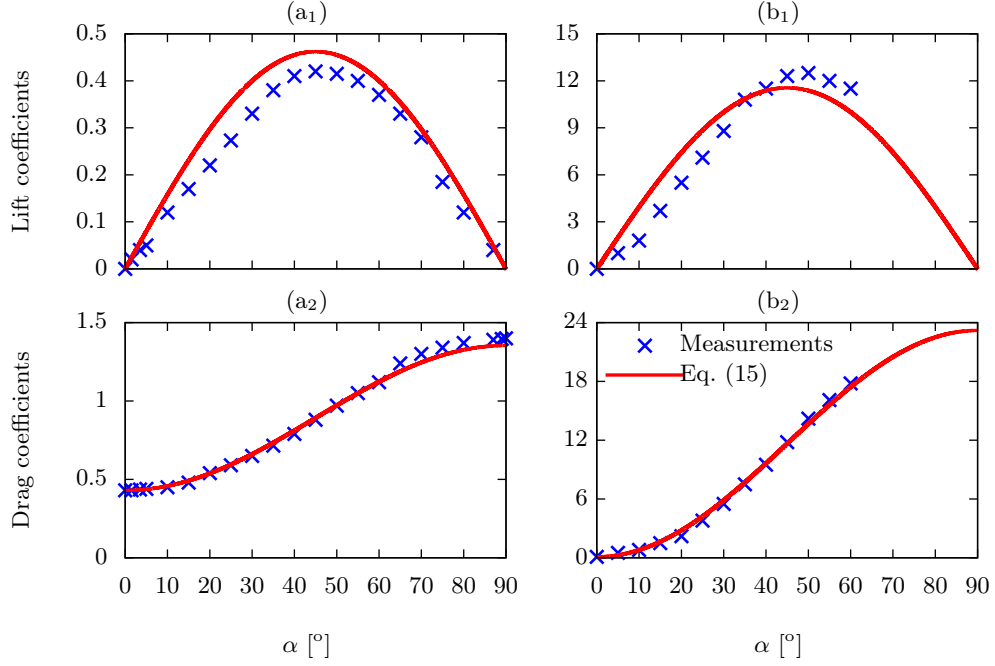


Figure 4: Aerodynamic coefficients of: (a_{1,2}) elliptic bodies; (b_{1,2}) missile-like bodies.

Proposition 2 *The functions C_D and C_L defined by*

$$C_D(\alpha) = c_0 + 2c_1 \sin^2(\alpha) \quad (15a)$$

$$C_L(\alpha) = c_1 \sin(2\alpha), \quad (15b)$$

with c_0 and c_1 two real numbers, satisfy the condition (12) with $C_{D_0} = c_0 + 2c_1$. The equivalent drag force and thrust intensity are then given by

$$\mathbf{F}_p(\mathbf{v}_a) = -k_a C_{D_0} |\mathbf{v}_a| \mathbf{v}_a, \quad (16a)$$

$$T_p = T + 2c_1 k_a |\mathbf{v}_a|^2 \cos(\alpha). \quad (16b)$$

The proof is straightforward. A particular bisymmetric body is the sphere whose aerodynamic characteristics (zero lift coefficient and constant drag coefficient) are obtained by setting $c_1 = 0$ in (15). Elliptic-shaped bodies are also bisymmetric but, in contrast with the sphere, they do generate lift in addition to drag. The process of approximating measured aerodynamic characteristics with functions given by (15) is illustrated by the Figure 4(a) where we have used experimental data borrowed from [17, p.19] for an elliptic-shaped body with Mach and Reynolds numbers equal to $M = 6$ and $Re = 7.96 \cdot 10^6$ respectively. For this example, the identified coefficients are $c_0 = 0.43$ and $c_1 = 0.462$. Since missile-like devices are “almost” bisymmetric, approximating their aerodynamic coefficients with such functions can also be attempted. For instance, the approximation shown in Figure 4(b) has been obtained by using experimental data taken from [38, p.54] for a missile moving at $M = 0.7$. In this case, the identified coefficients are $c_0 = 0.1$ and $c_1 = 11.55$. In both cases, the match between experimental data and the approximating functions, although far from perfect, should be sufficient for feedback control purposes.

Note that the process of approximating aerodynamics characteristics by trigonometric functions is not new (see, e.g., [5, 44]). To our knowledge, however, such approximations have not been exploited for the explicit determination of equilibrium orientations, as deduced from Proposition 1.

4 Control design

The results of the previous section are now exploited to address feedback control design of axisymmetric vehicles. We first start by considering the thrust direction control problem. Several solutions to this problem have already

been proposed in the literature. The solution proposed hereafter is a coordinate-free extension of the solution given in [12].

4.1 Thrust direction control

Consider a time-varying reference thrust (unitary) direction \mathbf{k}_r . It is assumed that \mathbf{k}_r varies smoothly with time so that $\dot{\mathbf{k}}_r(t)$ is well defined for any time t . The following result provides control expressions for the angular velocity control input $\boldsymbol{\omega}$ yielding a large stability domain.

Proposition 3 *The feedback law*

$$\boldsymbol{\omega} = \left(k_1(\mathbf{k}, t) + \frac{\dot{\gamma}(t)}{\gamma(t)} \right) \mathbf{k} \times \mathbf{k}_r + \boldsymbol{\omega}_r + \lambda(\mathbf{k}, t) \mathbf{k} \quad (17)$$

with $\boldsymbol{\omega}_r = \mathbf{k}_r \times \dot{\mathbf{k}}_r$, $\lambda(\cdot)$ any real-valued continuous function, $\gamma(\cdot)$ any smooth positive real-valued function such that $\inf_t \gamma(t) > 0$, and $k_1(\cdot)$ any continuous positive real-valued function such that $\inf_{\mathbf{k}, t} k_1(\mathbf{k}, t) > 0$, ensures exponential stability of the equilibrium $\mathbf{k} = \mathbf{k}_r$ with domain of attraction $\{\mathbf{k}(0) : \mathbf{k}(0) \cdot \mathbf{k}_r(0) \neq -1\}$.

The proof is given in the appendix.

The above expression of $\boldsymbol{\omega}$ is a generalization of the solution proposed in [12], for which the control gain γ was not present and a specific choice of k_1 was imposed. The additional degrees of freedom given by the above solution will be exploited further on. Recall that the limitation on the stability domain is due to the topology of the unit sphere, which forbids the existence of smooth autonomous feedback controllers yielding global asymptotic stability. The first term in the right-hand side of (17) is a nonlinear feedback term that depends on the error between \mathbf{k} and \mathbf{k}_r , here given by the cross product of these two vectors. The second term is a feedforward term. In practice, this term can be neglected when the vector $\dot{\mathbf{k}}_r$ (and thus $\boldsymbol{\omega}_r$) is not known, as in the case where \mathbf{k}_r corresponds to a reference thrust direction manually specified by a human pilot using a joystick. Omitting this feedforward term is not very damaging in terms of performance, provided that \mathbf{k}_r does not vary too rapidly. Finally, the last term in the right-hand side of (17) is associated with the rotation about the axis \mathbf{k} (yaw degree of freedom for a hovering VTOL vehicle, and roll degree of freedom for a missile or for a cruising airplane with annular wing). It does not affect the thrust direction dynamics since $\dot{\mathbf{k}} = \boldsymbol{\omega} \times \mathbf{k}$. Finally, let us comment on the choice of the control gains. Concerning $\lambda(\cdot)$, the simplest choice is obviously $\lambda(t) \equiv 0$. Another possibility is $\lambda(t) = -\boldsymbol{\omega}_r(t) \cdot \mathbf{k}(t)$. This yields $\boldsymbol{\omega}(t) \cdot \mathbf{k}(t) = 0 \forall t$ so that the control law does not induce any instantaneous rotation around \mathbf{k} . Other choices may be preferred when it matters to precisely control the vehicle's remaining rotational degree of freedom. Concerning γ and k_1 , a simple choice consists in taking constant positive numbers, but other possibilities can be preferable. For instance, taking $k_1(\mathbf{k}, t) = k_{1,0}/(1 + \mathbf{k} \cdot \mathbf{k}_r(t) + \epsilon_1)$, with $k_{1,0} > 0$ and ϵ_1 a small positive number, makes the feedback gain k_1 grow large when \mathbf{k} gets close to $-\mathbf{k}_r$ and, subsequently, tends to make this undesired equilibrium direction more repulsive. As for γ , a choice adapted to the objective of tracking reference trajectories, in either position or velocity, is pointed out thereafter.

4.2 Velocity and position control for axisymmetric vehicles

In what follows, $\mathbf{v}_r(\cdot)$ denotes a reference velocity time-function (at least three times differentiable everywhere). Velocity control then consists in the asymptotic stabilization of the velocity error $\tilde{\mathbf{v}} := \mathbf{v} - \mathbf{v}_r$ at zero. This control objective may be complemented by the convergence to zero of a position error $\tilde{\mathbf{p}} := \mathbf{p} - \mathbf{p}_r$, with $\mathbf{p}_r(\cdot)$ denoting a reference position time-function. In this latter case, \mathbf{v}_r is the time-derivative of \mathbf{p}_r , and the error state vector to be stabilized at zero contains the six-dimensional vector $(\tilde{\mathbf{p}}, \tilde{\mathbf{v}})$. The error vector may further include an integral of the position error $\tilde{\mathbf{p}}$. It is also possible that the application only requires the stabilization of the vehicle's altitude, in addition to its velocity. In order to take various control objectives involving the vehicle's velocity and possibly other state variables whose variations depends on this velocity, we consider from now on a "generalized" control objective consisting in the asymptotic stabilization at zero of an error vector denoted as $(\tilde{\boldsymbol{\rho}}, \tilde{\mathbf{v}})$, with $\tilde{\boldsymbol{\rho}} \in \mathbb{R}^p$ and such that $\dot{\tilde{\boldsymbol{\rho}}} = \mathbf{f}(\tilde{\boldsymbol{\rho}}, \tilde{\mathbf{v}})$, with $\mathbf{f}(\cdot, \cdot)$ denoting a smooth vector-valued function. For instance, in the case where $\tilde{\boldsymbol{\rho}} = \tilde{\mathbf{p}}$, with $\tilde{\mathbf{p}}$ denoting either a position error, or an integral of the velocity error $\tilde{\mathbf{v}}$, then $\mathbf{f}(\tilde{\boldsymbol{\rho}}, \tilde{\mathbf{v}}) = \tilde{\mathbf{v}}$. If $\tilde{\boldsymbol{\rho}} = (\mathbf{I}_p, \tilde{\mathbf{p}})$, with \mathbf{I}_p denoting a saturated integral of the position tracking error such that $\frac{d}{dt} \mathbf{I}_p = h(\tilde{\boldsymbol{\rho}})$, then $\mathbf{f}(\tilde{\boldsymbol{\rho}}, \tilde{\mathbf{v}}) = (h(\tilde{\boldsymbol{\rho}}), \tilde{\mathbf{v}})$. The simplest case corresponds to pure velocity control without integral correction, for which $\tilde{\boldsymbol{\rho}} = \emptyset$.

Consider now an axisymmetric vehicle with its velocity dynamics given by (13), and let $\mathbf{a}_r := \dot{\mathbf{v}}_r$ denote the reference acceleration. It follows from (13) that

$$m\dot{\tilde{\mathbf{v}}} = \mathbf{F}_p + m(\mathbf{g} - \mathbf{a}_r) - T_p \mathbf{k}. \quad (18)$$

Introducing an auxiliary feedback term $\boldsymbol{\xi}$, whose role and choice will be commented upon thereafter, this equation can be written as

$$m\dot{\tilde{\mathbf{v}}} = m\boldsymbol{\xi} + \bar{\mathbf{F}}_p - T_p \mathbf{k}, \quad (19)$$

with

$$\bar{\mathbf{F}}_p(\mathbf{v}_a, \mathbf{a}_r, \boldsymbol{\xi}) := \mathbf{F}_p(\mathbf{v}_a) + m(\mathbf{g} - \mathbf{a}_r - \boldsymbol{\xi}) \quad (20)$$

The idea is to end up working with the simple control system $\dot{\tilde{\mathbf{v}}} = \boldsymbol{\xi}$. To this aim Eq. (19) suggests to adopt a control strategy that ensures the convergence of $\bar{\mathbf{F}}_p - T_p \mathbf{k}$ to zero. With T_p preferred positive, this implies that the thrust direction \mathbf{k} should tend to

$$\mathbf{k}_r := \frac{\bar{\mathbf{F}}_p}{|\bar{\mathbf{F}}_p|}. \quad (21)$$

Recall from (14) that \mathbf{F}_p does not depend on \mathbf{k} . Thus, provided that $\boldsymbol{\xi}$ does not depend on \mathbf{k} , $\bar{\mathbf{F}}_p$ does not depend on \mathbf{k} either, and \mathbf{k}_r is well defined as long as $\bar{\mathbf{F}}_p$ does not vanish. This is precisely what makes Proposition 1 important for the control design. Convergence of $\bar{\mathbf{F}}_p - T_p \mathbf{k}$ to zero also implies that T_p must tend to $\bar{\mathbf{F}}_p \cdot \mathbf{k}$. From (6) and (13), this is equivalent to the convergence of the thrust intensity T to $\bar{\mathbf{F}}_a \cdot \mathbf{k}$ with

$$\bar{\mathbf{F}}_a := \mathbf{F}_a + m(\mathbf{g} - \mathbf{a}_r - \boldsymbol{\xi}) \quad (22)$$

Once the reference thrust direction \mathbf{k}_r is properly defined, a possible control law, among other possibilities, is pointed out in the following proposition.

Proposition 4 *Consider an axisymmetric vehicle for which the aerodynamic characteristics satisfy relation (12), and a smooth feedback controller $\boldsymbol{\xi}(\tilde{\boldsymbol{\rho}}, \tilde{\mathbf{v}})$ for the control system*

$$\dot{\tilde{\boldsymbol{\rho}}} = \mathbf{f}(\tilde{\boldsymbol{\rho}}, \tilde{\mathbf{v}}) \quad (23a)$$

$$\dot{\tilde{\mathbf{v}}} = \boldsymbol{\xi} \quad (23b)$$

Assume that

A1 : $\boldsymbol{\xi}(\tilde{\boldsymbol{\rho}}, \tilde{\mathbf{v}})$ makes $(\tilde{\boldsymbol{\rho}}, \tilde{\mathbf{v}}) = (\mathbf{0}, \mathbf{0})$ a locally exponentially stable equilibrium point of System (23);

A2 : $\bar{\mathbf{F}}_p$ does not vanish along the velocity reference trajectory \mathbf{v}_r , i.e., $\exists \delta > 0 : \delta \leq \bar{\mathbf{F}}_p(\mathbf{v}_{r,a}(t), \mathbf{a}_r(t), \mathbf{0}), \forall t$, with $\mathbf{v}_{r,a} := \mathbf{v}_r - \mathbf{v}_w$.

Then, $T = \bar{\mathbf{F}}_a \cdot \mathbf{k}$ and $\boldsymbol{\omega}$ given by (17), with \mathbf{k}_r defined by (21), $\gamma = \sqrt{c_2 + |\bar{\mathbf{F}}_p|^2}$, and c_2 any strictly positive constant, ensure local exponential stability of the equilibrium point $(\tilde{\boldsymbol{\rho}}, \mathbf{v}, \mathbf{k}) = (\mathbf{0}, \mathbf{v}_r, \mathbf{k}_r)$ for the system (23a)-(6).

The proof is given in the appendix.

Let us comment on the above result.

1. Proposition 4 essentially shows how to derive an exponentially stabilizing feedback law for the underactuated System (6) from an exponentially stabilizing feedback controller for the fully-actuated system $\dot{\tilde{\mathbf{v}}} = \boldsymbol{\xi}$. Since feedback control of fully-actuated systems can be addressed with a large variety of existing control laws, starting with linear feedback control, the determination of $\boldsymbol{\xi}$ will not be further addressed here.
2. Once an exponential stabilizer $\boldsymbol{\xi}$ of the origin of System (23) is determined, local exponential stability of zero tracking errors for an antisymmetric vehicle for which the aerodynamic characteristics satisfy relation (12) essentially relies on Assumption 2, which imposes that the reference thrust direction \mathbf{k}_{ref} , associated with perfect tracking of the reference trajectory, is well defined at all times. This condition may be violated for very specific and aggressive reference trajectories. Note, however, that its satisfaction can be checked from the knowledge of the reference velocity only (assuming of course that an accurate model of aerodynamic forces is available).

3. Finally, let us discuss a few issues related to the calculation of the feedback control. The main difficulty at this level comes from the fact that both \mathbf{k}_r and γ depend on $\bar{\mathbf{F}}_p$. Since $\dot{\gamma}$ and $\dot{\mathbf{k}}_r$ are involved in the calculation of $\boldsymbol{\omega}$, the time-derivative of $\bar{\mathbf{F}}_p$ has to be calculated also. In practice, a possibility consists in estimating this term, e.g. from the calculation of $\bar{\mathbf{F}}_p$ and using a high-gain observer. Another possible choice, consisting in using the reference velocity instead of the vehicle's actual velocity to calculate an approximation of this term, is made for the simulations reported in the next section.

Proposition 4 guarantees *local* asymptotic stability only. The difficulty to ensure a large domain of convergence comes from the risk of $\bar{\mathbf{F}}_p$ vanishing at some point, which would in turn make \mathbf{k}_r , as specified by (21), ill-defined. This risk, although small, cannot be ruled out in the most general situation, especially because the term \mathbf{F}_p in $\bar{\mathbf{F}}_p$ (i.e. the term resulting from the aerodynamic forces acting on the vehicle) can take very large values. In practice, the necessity of having a control always well defined implies that one has to modify the term $\bar{\mathbf{F}}_p$ used in the control expression in order to avoid its passage through zero. A reasonable way of making this modification is a subject of future studies. Taking the above-mentioned difficulty aside, if one assumes that $\bar{\mathbf{F}}_p$ remains different from zero, then convergence of the tracking errors can be guaranteed, as specified by the following proposition.

Proposition 5 *Given the feedback law of Proposition 4, if one further assumes that*

A1(bis) : $\xi(\tilde{\boldsymbol{\rho}}, \tilde{\mathbf{v}})$ *globally asymptotically stabilizes the origin* $(\tilde{\boldsymbol{\rho}}, \tilde{\mathbf{v}}) = (\mathbf{0}, \mathbf{0})$ *of the system*

$$\begin{aligned}\dot{\tilde{\boldsymbol{\rho}}} &= \mathbf{f}(\tilde{\boldsymbol{\rho}}, \tilde{\mathbf{v}}) \\ \dot{\tilde{\mathbf{v}}} &= \xi(\tilde{\boldsymbol{\rho}}, \tilde{\mathbf{v}}) + \varepsilon(t)\end{aligned}$$

when the "perturbation" $\varepsilon(\cdot)$ is identically zero, and still ensures the convergence to zero of the solutions to this system when $\varepsilon(\cdot)$ converges to zero exponentially;

then any solution to the closed-loop system (23a)-(6) along which $\bar{\mathbf{F}}_p$ does not vanish (in the sense that $\exists \delta > 0 : \delta \leq \bar{\mathbf{F}}_p(\mathbf{v}_a(t), \mathbf{a}_r(t), \xi(\tilde{\boldsymbol{\rho}}, \tilde{\mathbf{v}})), \forall t$) converges to the equilibrium point $(\mathbf{0}, \mathbf{v}_r, \mathbf{k}_r)$.

The proof follows directly from the proof of Proposition 4. Preservation of the convergence to zero of the system's solutions in the case of an exponentially decaying additive perturbation, although needed for the sake of completeness, is a weak requirement that has little impact on the control design.

4.3 Simulation results

The feedback law of Proposition 4 is applied to a model of the C-701 anti-ship missile, whose geometry and operational characteristics are close to those of the device associated with the measured aerodynamic coefficients of Figure 4(b). The control objective is the asymptotic stabilization at zero of the velocity error $\tilde{\mathbf{v}}$. A saturated integral $\tilde{\boldsymbol{\rho}} = \mathbf{I}_v$ of this error is used in the control law in order to compensate for static modelling errors and additive perturbations. This integral term is obtained as the (numerical) solution to the following equation [22] [37]

$$\frac{d}{dt} \mathbf{I}_v = \mathbf{f}(\tilde{\boldsymbol{\rho}}, \tilde{\mathbf{v}}) = -k_I \mathbf{I}_v + k_I \text{sat}^\delta \left(\mathbf{I}_v + \frac{\tilde{\mathbf{v}}}{k_I} \right) ; \mathbf{I}_v(0) = \mathbf{0}, \quad (24)$$

with k_I a (not necessarily constant) positive number characterizing the desaturation rate, $\delta > 0$ the upperbound of $|\mathbf{I}_v|$, and sat^δ a differentiable approximation of the classical saturation function defined by $\text{sat}^\delta(\mathbf{x}) = \min \left(1, \frac{\delta}{|\mathbf{x}|} \right) \mathbf{x}$. The feedback law of Proposition 4 is then applied with

$$\begin{aligned}\xi(\tilde{\boldsymbol{\rho}}, \tilde{\mathbf{v}}) &= -k_v \tilde{\mathbf{v}} - k_i \mathbf{I}_v, \\ k_1(\mathbf{k}, t) &= k_{1,0} / (1 + \mathbf{k} \cdot \mathbf{k}_r(t) + \epsilon_1)^2, \\ \lambda(\mathbf{k}, t) &= -\boldsymbol{\omega}_r(t) \cdot \mathbf{k}(t),\end{aligned} \quad (25)$$

and with $k_v = 5$, $k_i = k_v^2/4$, $k_I = 50$, $k_{1,0} = 10$, $\epsilon_1 = 0.01$. The feedforward term $\boldsymbol{\omega}_r$ is evaluated using the reference acceleration $\dot{\mathbf{v}}_r$ rather than the vehicle's acceleration $\dot{\mathbf{v}}$ calculated from Newton's equation (6) and the model of aerodynamic forces \mathbf{F}_a used for control design.

The simulated vehicle's equations of motion are given by (6)-(8), with the aerodynamic coefficients $C_L(\alpha)$ and $C_D(\alpha)$ obtained by interpolating the measurements reported in [38, p.54] (see Figure 4(b)). These coefficients thus differ from the approximating functions (15) used in the control calculation. The values of the parameters

involved in these functions are the identified values reported previously, i.e. $c_0 = 0.1$ and $c_1 = 11.55$. The missile's physical parameters are $m = 100$ [Kg] and $(\rho, \Sigma) = (1.292, 0.5)$ ($[Kg/m^3]$, $[m]^2$), so that $k_a \approx 0.3$ [Kg/m]. These values are replaced by estimated ones, namely $\hat{k}_a = 0.24$ and $\hat{m} = 80$ [Kg], in the control calculation in order to test the control robustness w.r.t. parametric uncertainties. In particular, the vector $\bar{\mathbf{F}}_p$ in (20) is calculated with $\mathbf{F}_p(\mathbf{v}_a) = -\hat{k}_a(c_0 + 2c_1)|\mathbf{v}_a|\mathbf{v}_a$.

The reference velocity $\mathbf{v}_r(t)$, expressed in Mach numbers (1 *Mach* = 340 [m/sec]), is piece-wise constant on the time interval $[0, 40)$ [sec], and continuously time-varying on the time interval $[40, 60)$ [sec]. More precisely:

$$\mathbf{v}_r(t) = \begin{cases} 0.7\mathbf{i}_0 & 0 \leq t < 10, \\ -0.7\mathbf{j}_0 & 10 \leq t < 20, \\ -0.7\mathbf{k}_0 & 20 \leq t < 30, \\ -0.7\mathbf{i}_0 & 30 \leq t < 40, \end{cases} \quad (26)$$

and $\mathbf{v}_r(t) = -0.5 \sin(t\pi/5)\mathbf{i}_0 + 0.6 \sin(t\pi/10)\mathbf{j}_0 + 0.6 \cos(t\pi/10)\mathbf{k}_0$ when $40 \leq t < 60$. The applied thrust force and angular velocity $\boldsymbol{\omega} = (\mathbf{i}, \mathbf{j}, \mathbf{k})\omega$ are saturated as follows:

$$\begin{aligned} 0 &< T < 10\hat{m}g, \\ |\omega_i| &< 2\pi, \quad i = \{1, 2, 3\}. \end{aligned} \quad (27)$$

The initial velocity and attitude are: $\mathbf{v}(0) = 0.5\mathbf{i}_0$ [Mach], $\phi_0 = \psi_0 = 0^\circ$, $\theta_0 = -40^\circ$ where (ϕ, θ, ψ) denote standard *roll*, *pitch*, and *yaw* angles as defined in [40, p. 47].

From top to bottom, Figure 5 shows the time-evolution of the reference velocity $\mathbf{v}_r = (\mathbf{i}_0, \mathbf{j}_0, \mathbf{k}_0)\dot{x}_r$, the vehicle's velocity $\mathbf{v} = (\mathbf{i}_0, \mathbf{j}_0, \mathbf{k}_0)\dot{x}$, the angle of attack α , the angular velocity $\boldsymbol{\omega} = (\mathbf{i}, \mathbf{j}, \mathbf{k})\omega$, the applied thrust-to-weight ratio, the norm of the vector $\bar{\mathbf{F}}_p$ (which has to remain different from zero to ensure the well-posedness of the control solution), and the angle $\tilde{\theta}$ between the thrust direction \mathbf{k} and the reference direction \mathbf{k}_r . There is no wind. The initial angle of attack at $t = 0$ is 50° . The attitude control makes this angle decrease rapidly. Sharp discontinuities of the reference velocity at the time instants $t = 10, 20, 30, 40$ [sec] are responsible for the observable transitions and temporarily large angles of attack. Thanks to the integral correction terms resulting from the use of \mathbf{I}_v in the control law, the velocity error converges to zero when the reference velocity is constant. On the time interval $[40, 60)$ [sec], despite rapidly varying reference velocities, velocity errors are ultimately small, thanks to the combination of pre-compensation and integral correction terms that are present in the control law.

Figure 6 illustrates the improvement brought by the control design proposed in this paper w.r.t. a nonlinear control design that does not take the dependence of the aerodynamic forces upon the vehicle's orientation into account. To this aim, we consider the velocity control proposed in [12] for spherical-like vehicles subjected to aerodynamic drag solely. The comparison is facilitated by the fact that this control is basically the same as the one considered in Proposition 4 with $\bar{\mathbf{F}}_a$ used in place of $\bar{\mathbf{F}}_p$ in the control law. Figure 6 shows the evolution of $|\bar{\mathbf{F}}_a|$ and $\tilde{\theta}$ when applying this control, with the feedforward term $\boldsymbol{\omega}_r$ (whose calculation involves $\dot{\bar{\mathbf{F}}}_a$) set equal to zero for the sake of simplification. One can observe from this figure that i) relative variations of the norm of $|\bar{\mathbf{F}}_a|$ are significantly more pronounced than those of $|\bar{\mathbf{F}}_p|$ in Figure 5 (a consequence of the dependence of $\bar{\mathbf{F}}_a$ upon the vehicle's orientation), ii) the amplitude of the orientation error $\tilde{\theta}$ after a discontinuous change of the reference velocity is much more important (an indication of degraded performance), and, even more significantly iii) $\bar{\mathbf{F}}_a$ crosses zero little after the reference velocity discontinuity occurring at $t = 40$ [sec], with the brisk consequence that the reference direction \mathbf{k}_r , and thus the control law, are not defined at this point (thus leading to an abrupt stop of the simulation).

5 Conclusion and perspectives

Extension of the thrust direction control paradigm to a class of vehicles with axisymmetric body shapes has been addressed. Application examples include, e.g., rockets and aerial vehicles using annular wings for the production of lift. Specific aerodynamic properties associated with these particular shapes allow for the design of nonlinear feedback controllers yielding asymptotic stability in a very large flight envelope. Further extension of the present approach to vehicles with non-symmetric body shapes (e.g. conventional airplanes) is currently investigated in relation to a better understanding of the control limitations induced by the stall phenomenon (see e.g. [33] for a preliminary study on this latter issue). Clearly, the control solution here proposed calls for a multitude of

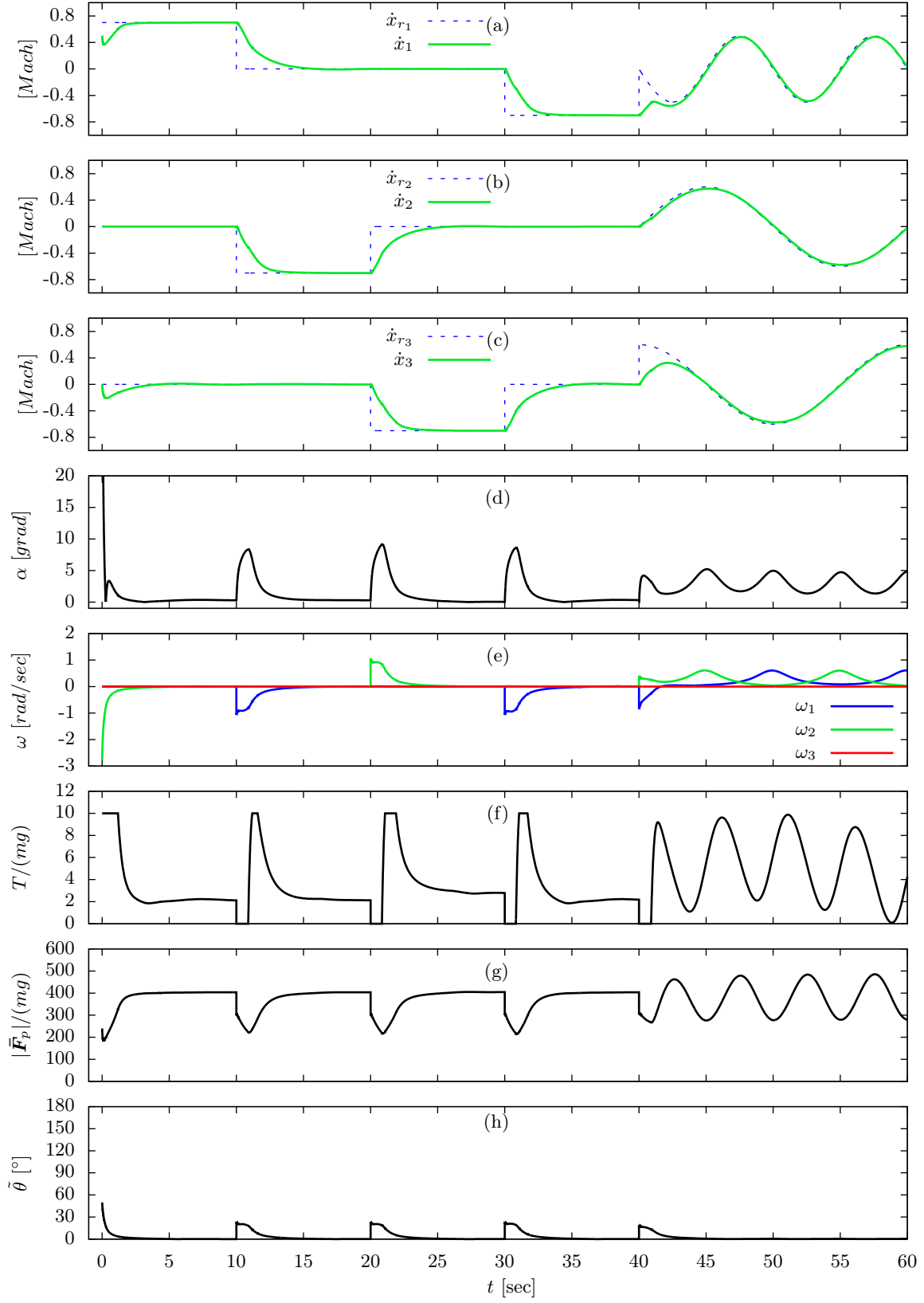


Figure 5: Simulation of a C-701 trajectory with \bar{F}_p in angular control.

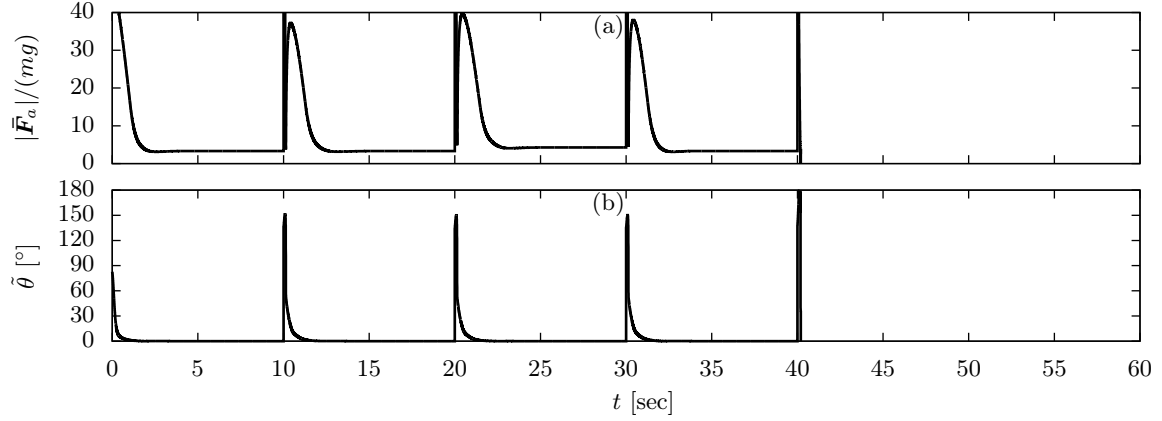


Figure 6: Simulation of a C-701 trajectory with \bar{F}_a in angular control.

complementary extensions and adaptations before it is implemented on a physical device. Let us just mention the production of control torques allowing for desired angular velocity changes, and the determination of corresponding low level control loops that take actuators' physical limitations into account –in relation, for instance, to the airspeed dependent control authority associated with the use of flaps and rudders. The addition of actuation degrees of freedom via thrust direction "vectoring" in order, for instance, to decouple vehicle's attitude control from the constraint of thrust direction alignment with the sum of external forces acting on the vehicle, constitutes another extension of the present study.

Appendix

We will make use of the following classical vectorial relations:

$$\begin{aligned} \forall \mathbf{x}, \mathbf{y}, \mathbf{z} \in \mathbf{E}^3, \quad & \mathbf{x} \cdot (\mathbf{y} \times \mathbf{z}) = \mathbf{y} \cdot (\mathbf{z} \times \mathbf{x}) \\ \forall \mathbf{x}, \mathbf{y}, \mathbf{z} \in \mathbf{E}^3, \quad & \mathbf{x} \times (\mathbf{y} \times \mathbf{z}) = (\mathbf{x} \cdot \mathbf{z})\mathbf{y} - (\mathbf{x} \cdot \mathbf{y})\mathbf{z} \end{aligned} \quad (28)$$

Proof of Proposition 3

Consider the function $V_0 := 1 - \mathbf{k} \cdot \mathbf{k}_r$ and note that V_0 is non-negative and vanishes only when $\mathbf{k} = \mathbf{k}_r$. Recall that $\boldsymbol{\omega}_r = \dot{\mathbf{k}}_r \times \mathbf{k}_r$. By using (28) and the fact that \mathbf{k}_r is a unit vector, one deduces that $\dot{\mathbf{k}}_r = \boldsymbol{\omega}_r \times \mathbf{k}_r$. The time-derivative of V_0 thus satisfies:

$$\begin{aligned} \dot{V}_0 &= -\dot{\mathbf{k}} \cdot \mathbf{k}_r - \mathbf{k} \cdot \dot{\mathbf{k}}_r \\ &= -(\boldsymbol{\omega} \times \mathbf{k}) \cdot \mathbf{k}_r - \mathbf{k} \cdot (\boldsymbol{\omega}_r \times \mathbf{k}_r) \\ &= (\boldsymbol{\omega}_r - \boldsymbol{\omega}) \cdot (\mathbf{k} \times \mathbf{k}_r) \end{aligned} \quad (29)$$

where the last equality follows from (28). Now, define

$$\begin{aligned} V_1 &:= \frac{\gamma^2(t)}{2} \frac{1 - \mathbf{k} \cdot \mathbf{k}_r}{1 + \mathbf{k} \cdot \mathbf{k}_r} \\ &= \frac{\gamma^2(t)}{2} \frac{1 - (\mathbf{k} \cdot \mathbf{k}_r)^2}{(1 + \mathbf{k} \cdot \mathbf{k}_r)^2} \\ &= \frac{\gamma^2(t)}{2} \frac{|\mathbf{k} \times \mathbf{k}_r|^2}{(1 + \mathbf{k} \cdot \mathbf{k}_r)^2} \end{aligned} \quad (30)$$

where the third equality comes from that $(\mathbf{k} \cdot \mathbf{k}_r)^2 + |\mathbf{k} \times \mathbf{k}_r|^2 = 1$, since \mathbf{k} and \mathbf{k}_r are unit vectors. Note also that $V_1 = \frac{1}{2}\gamma^2(t)\tan^2(\frac{\tilde{\theta}}{2})$ where $\tilde{\theta}$ is the angle between the vectors \mathbf{k} and \mathbf{k}_r . One verifies that

$$\dot{V}_1 = \gamma(t)\dot{\gamma}(t)\frac{1 - \mathbf{k} \cdot \mathbf{k}_r}{1 + \mathbf{k} \cdot \mathbf{k}_r} + \gamma^2(t)\frac{\dot{V}_0}{(1 + \mathbf{k} \cdot \mathbf{k}_r)^2}$$

and it follows from (29) and (30) that

$$\begin{aligned}\dot{V}_1 &= \gamma(t)\dot{\gamma}(t)\frac{|\mathbf{k} \times \mathbf{k}_r|^2}{(1 + \mathbf{k} \cdot \mathbf{k}_r)^2} + \gamma^2(t)\frac{(\mathbf{k} \times \mathbf{k}_r) \cdot (\boldsymbol{\omega}_r - \boldsymbol{\omega})}{(1 + \mathbf{k} \cdot \mathbf{k}_r)^2} \\ &= \gamma(t)\frac{\mathbf{k} \times \mathbf{k}_r}{(1 + \mathbf{k} \cdot \mathbf{k}_r)^2}(\dot{\gamma}(t)\mathbf{k} \times \mathbf{k}_r + \gamma(t)(\boldsymbol{\omega}_r - \boldsymbol{\omega}))\end{aligned}\quad (31)$$

Replacing $\boldsymbol{\omega}$ by its expression (17) yields

$$\begin{aligned}\dot{V}_1 &= -k_1(\mathbf{k}, t)\gamma^2(t)\frac{|\mathbf{k} \times \mathbf{k}_r|^2}{(1 + \mathbf{k} \cdot \mathbf{k}_r)^2} \\ &= -2k_1(\mathbf{k}, t)V_1\end{aligned}\quad (32)$$

Since $k_1(\cdot)$ is, by assumption, lower-bounded by a positive scalar, V_1 converges exponentially to zero. Exponential stability of $\mathbf{k} = \mathbf{k}_r$ then follows from the definition of V_1 and the fact that $\gamma(\cdot)$ is lower-bounded by a positive scalar.

Proof of Proposition 4

First, note that in view of Assumption 2 the vector \mathbf{k}_r is well defined in a neighborhood of the equilibrium point $(\tilde{\boldsymbol{\rho}}, \tilde{\mathbf{v}}, \mathbf{k}) = (\mathbf{0}, \mathbf{v}_r, \mathbf{k}_r)$. Then, the term $\gamma(t)$ in (17) is lower-bounded by $\sqrt{c_1} > 0$. Therefore, the feedback law is well defined in a neighborhood of the equilibrium point.

From (6) and (13), $\mathbf{F}_p - T_p\mathbf{k} = \mathbf{F}_a - T\mathbf{k}$. Therefore $\bar{\mathbf{F}}_p - T_p\mathbf{k} = \bar{\mathbf{F}}_a - T\mathbf{k}$ and

$$\begin{aligned}\bar{\mathbf{F}}_p \cdot \mathbf{k} &= T_p - T + \bar{\mathbf{F}}_a \cdot \mathbf{k} \\ &= T_p\end{aligned}$$

From this relation and (21), Eq. (19) can be written as follows:

$$\begin{aligned}m\dot{\tilde{\mathbf{v}}} &= |\bar{\mathbf{F}}_p|\mathbf{k}_r - T_p\mathbf{k} + m\xi(\tilde{\boldsymbol{\rho}}, \tilde{\mathbf{v}}) \\ &= |\bar{\mathbf{F}}_p|\mathbf{k}_r - (\bar{\mathbf{F}}_p \cdot \mathbf{k})\mathbf{k} + m\xi(\tilde{\boldsymbol{\rho}}, \tilde{\mathbf{v}}) \\ &= |\bar{\mathbf{F}}_p|\mathbf{k}_r - (|\bar{\mathbf{F}}_p|\mathbf{k}_r \cdot \mathbf{k})\mathbf{k} + m\xi(\tilde{\boldsymbol{\rho}}, \tilde{\mathbf{v}}) \\ &= |\bar{\mathbf{F}}_p|(\mathbf{k}_r - (\mathbf{k}_r \cdot \mathbf{k})\mathbf{k}) + m\xi(\tilde{\boldsymbol{\rho}}, \tilde{\mathbf{v}}) \\ &= |\bar{\mathbf{F}}_p|(\mathbf{k} \times (\mathbf{k}_r \times \mathbf{k})) + m\xi(\tilde{\boldsymbol{\rho}}, \tilde{\mathbf{v}})\end{aligned}\quad (33)$$

where the last equality comes from (28). Therefore, along the solutions to the controlled system, the variables $\tilde{\boldsymbol{\rho}}$ and $\tilde{\mathbf{v}}$ satisfy the following relations:

$$\begin{aligned}\dot{\tilde{\boldsymbol{\rho}}} &= \mathbf{f}(\tilde{\boldsymbol{\rho}}, \tilde{\mathbf{v}}) \\ \dot{\tilde{\mathbf{v}}} &= \xi(\tilde{\boldsymbol{\rho}}, \tilde{\mathbf{v}}) + \varepsilon\end{aligned}\quad (34)$$

with the "additive perturbation" ε defined by

$$\varepsilon := \frac{1}{m}|\bar{\mathbf{F}}_p|(\mathbf{k} \times (\mathbf{k}_r \times \mathbf{k}))$$

From the definition of $\boldsymbol{\omega}$ and Proposition 3, \mathbf{k} converges to \mathbf{k}_r exponentially. More precisely, from the proof of Proposition 3, the function V_1 defined by (30) converges to zero exponentially. Since \mathbf{k} and \mathbf{k}_r are unit vectors, it follows from (30) and the definition of γ that

$$\begin{aligned}V_1 &\geq \frac{\gamma^2(t)}{8}|\mathbf{k} \times \mathbf{k}_r|^2 \\ &\geq \frac{|\bar{\mathbf{F}}_p|^2}{8}|\mathbf{k} \times \mathbf{k}_r|^2 \\ &\geq \frac{|\bar{\mathbf{F}}_p|^2}{8}|\mathbf{k} \times (\mathbf{k} \times \mathbf{k}_r)|^2 \\ &\geq \frac{8}{m^2}|\varepsilon|^2 \\ &\geq \frac{8}{m^2}\end{aligned}$$

Therefore,

$$\varepsilon \leq \frac{\sqrt{8V_1}}{m}\quad (35)$$

so that ε also converges to zero exponentially. From Assumption 1 and converse Lyapunov theorems (See, e.g., [18, Section 4.7]) there exists a quadratic Lyapunov function $V_2(\tilde{\rho}, \tilde{v})$ for System (23), i.e., such that in a neighborhood of $(\tilde{\rho}, \tilde{v}) = (\mathbf{0}, \mathbf{0})$,

$$\dot{V}_2(\tilde{\rho}, \tilde{v}) \leq -k_2 V_2(\tilde{\rho}, \tilde{v}) \quad (36)$$

Using the triangular inequality, it follows from (32), (34), (35), and (36) that the function

$$V = \alpha V_1 + V_2$$

is a Lyapunov function for the controlled system for $\alpha > 0$ large enough.

References

- [1] J.D. Anderson. *Fundamentals of Aerodynamics*. McGraw Hill Series in Aeronautical and Aerospace Engineering, 5nd ed edition, 2010.
- [2] S. Bertrand, H. Piet-Lahanier, and T. Hamel. Contractive model predictive control of an unmanned aerial vehicle model. In *17th IFAC Symp. on Automatic Control in Aerospace*, volume 17, 2007.
- [3] S. Bouabdallah and R. Siegwart. Backstepping and sliding-mode techniques applied to an indoor micro quadrotor. In *IEEE International Conference on Robotics and Automation*, 2005.
- [4] P.J. Bristeau, P. Martin, and E. Salaun. The role of propeller aerodynamics in the model of a quadrotor UAV. In *European Control Conference*, pages 683–688, 2009.
- [5] M.H. Dickinson, F.-O. Lehmann, and S.P. Sane. Wing rotation and the aerodynamics basis of insect flight. *Science*, pages 1954–1960, 1999.
- [6] A. Dzul, T. Hamel, and R. Lozano. Modeling and nonlinear control for a coaxial helicopter. In *IEEE Conf. on Systems, Man and Cybernetics*, volume 6, 2002.
- [7] T. I. Fossen. *Guidance and control of ocean vehicles*. John Wiley and Sons, 1994.
- [8] N. Guenard, T. Hamel, and V. Moreau. Dynamic modeling and intuitive control strategy for an "x4-flyer". In *International Conference on Control and Automation (ICCA2005)*, pages 141–146, 2005.
- [9] T. Hamel, R. Mahony, R. Lozano, and J. Ostrowski. Dynamic modelling and configuration stabilization for an X4-flyer. In *IFAC World Congress*, pages 200–212, 2002.
- [10] J. Hauser, S. Sastry, and G. Meyer. Nonlinear control design for slightly non-minimum phase systems: Application to V/STOL. *Automatica*, 28:651–670, 1992.
- [11] M.-D. Hua. *Contributions to the Automatic Control of Aerial Vehicles*. PhD thesis, Université de Nice-Sophia Antipolis, 2009. Available at <http://hal.archives-ouvertes.fr/tel-00460801/>.
- [12] M.-D. Hua, T. Hamel, P. Morin, and C. Samson. A control approach for thrust-propelled underactuated vehicles and its application to VTOL drones. *IEEE Trans. on Automatic Control*, 54(8):1837–1853, 2009.
- [13] M.-D. Hua, T. Hamel, P. Morin, and C. Samson. Introduction to feedback control of underactuated vtol vehicles. *IEEE Control Systems Magazine*, pages 61–75, 2013.
- [14] H. Huang, G. M. Hoffmann, S. L. Waslander, and C. J. Tomlin. Aerodynamics and Control of Autonomous Quadrotor Helicopters in Aggressive Maneuvering. In *IEEE Conf. on Robotics and Automation*, pages 3277–3282, 2009.
- [15] A. Isidori, L. Marconi, and A. Serrani. *Robust autonomous guidance: an internal-model based approach*. Springer Verlag, 2003.
- [16] E. N. Johnson and M. A. Turbe. Modeling, control, and flight testing of a small ducted fan aircraft. *Journal of Guidance, Control, and Dynamics*, 29(4):769–779, 2006.

- [17] J. W. Keyes. Aerodynamic characteristics of lenticular and elliptic shaped configurations at a mach number of 6. Technical Report NASA-TN-D-2606, NASA, 1965.
- [18] H.K. Khalil. *Nonlinear systems*. Prentice Hall, third edition, 2002.
- [19] H. J. Kim, D. H. Shim, and S. Sastry. Nonlinear model predictive tracking control for rotorcraft-based unmanned aerial vehicles. In *American Control Conference*, pages 3576–3581, 2002.
- [20] A. Ko, O. J. Ohanian, and P. Gelhausen. Ducted fan UAV modeling and simulation in preliminary design. In *AIAA Modeling and Simulation Technologies Conference and Exhibit*, pages 2007–6375, 2007.
- [21] T. J. Koo and S. Sastry. Output tracking control design for a helicopter model based on approximate linearization. In *IEEE Conf. on Decision and Control*, pages 3635–3640, 1998.
- [22] C. Samson M.-D. Hua. Time sub-optimal nonlinear pi and pid controllers applied to longitudinal headway car control. *Int. J. of Control*, 84-10:1717–1728, 2011.
- [23] R. Mahony, T. Hamel, and A. Dzul. Hover control via an approximate lyapunov control for a model helicopter. In *IEEE Conf. on Decision and Control*, pages 3490–3495, 1999.
- [24] L. Marconi, A. Isidori, and A. Serrani. Autonomous vertical landing on an oscillating platform: an internal-model based approach. *Automatica*, 38:21–32, 2002.
- [25] E. Muir. Robust flight control design challenge problem formulation and manual: The high incidence research model (hirm). In *Robust Flight Control, A Design Challenge (GARTEUR)*, volume 224 of *Lecture Notes in Control and Information Sciences*, pages 419–443. Springer Verlag, 1997.
- [26] R. Naldi. *Prototyping, Modeling and Control of a Class of VTOL Aerial Robots*. PhD thesis, University of Bologna, 2008.
- [27] R. Olfati-Saber. *Nonlinear Control of Underactuated Mechanical Systems with Application to Robotics and Aerospace vehicles*. PhD thesis, Massachusetts Institute of Technology, 2001.
- [28] J.-M. Pflimlin. *Commande d’un minidrone à hélice carénée: de la stabilisation dans le vent à la navigation autonome (in French)*. PhD thesis, Ecole Doctorale Systèmes de Toulouse, 2006.
- [29] J.-M. Pflimlin, P. Binetti, P. Souères, T. Hamel, and D. Trouchet. Modeling and attitude control analysis of a ducted-fan micro aerial vehicle. *Control Engineering Practice*, pages 209–218, 2010.
- [30] J.-M. Pflimlin, P. Souères, and T. Hamel. Hovering flight stabilization in wind gusts for ducted fan UAV. In *IEEE Conf. on Decision and Control*, pages 3491–3496, 2004.
- [31] P. Pounds, R. Mahony, and P. Corke. Modelling and control of a large quadrotor robot. *Control Engineering Practice*, pages 691–699, 2010.
- [32] R.W. Prouty. *Helicopter Performance, Stability, and Control*. Krieger, 2005.
- [33] D. Pucci. Flight dynamics and control in relation to stall. In *American Control Conf. (ACC)*, pages 118–124, 2012.
- [34] D. Pucci. *Towards a unified approach for the control of aerial vehicles*. PhD thesis, Université de Nice-Sophia Antipolis and “Sapienza” Università di Roma, 2013.
- [35] D. Pucci, T. Hamel, P. Morin, and C. Samson. Modeling for control of symmetric aerial vehicles subjected to aerodynamic forces. *arXiv*, 2012.
- [36] C. Roos, C. Döll, and J.-M. Biannic. Flight control laws: recent advances in the evaluation of their robustness properties. *Aerospace Lab*, 2012.
- [37] H. Khalil S. Seshagiri. Robust output feedback regulation of minimum-phase nonlinear systems using conditional integrators. *Automatica*, 41:43–54, 2005.

- [38] B. F. Saffel, M. L. Howard, and E. N. Brooks. A method for predicting the static aerodynamic characteristics of typical missile configurations for angles of attack to 180 degrees. Technical Report AD0729009, Department of the navy naval ship research and development center, 1971.
- [39] S. N. Singh and A. Schy. Output feedback nonlinear decoupled control synthesis and observer design for maneuvering aircraft. *International Journal of Control*, 31(31):781–806, 1980.
- [40] R. F. Stengel. *Flight Dynamics*. Princeton University Press, 2004.
- [41] B. L. Stevens and F. L. Lewis. *Aircraft Control and Simulation*. Wiley-Interscience, 2nd ed edition, 2003.
- [42] J. C. A. Vilchis, B. Brogliato, A. Dzul, and R. Lozano. Nonlinear modelling and control of helicopters. *Automatica*, 39:1583–1596, 2003.
- [43] Q. Wang and R.F. Stengel. Robust nonlinear flight control of high-performance aircraft. *IEEE Transactions on Control Systems Technology*, 13(1):15–26, 2005.
- [44] Z.J. Wang. Aerodynamic efficiency of flapping flight: analysis of a two-stroke model. *The journal of experimental biology*, pages 234–238, 2008.
- [45] R. Xu and U. Ozguner. Sliding mode control of a class of underactuated systems. *Automatica*, 44:233–241, 2008.